

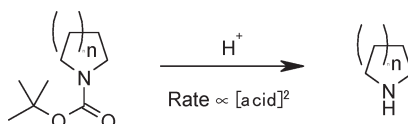
Kinetics and Mechanism of *N*-Boc Cleavage: Evidence of a Second-Order Dependence upon Acid Concentration

Ian W. Ashworth,* Brian G. Cox, and Brian Meyrick

Pharmaceutical Development, AstraZeneca R&D, S41/18 PR&D Building, Silk Road Business Park, Charter Way, Macclesfield, Cheshire, SK10 2NA, United Kingdom

ian.ashworth@astrazeneca.com

Received September 8, 2010



The kinetics of the HCl-catalyzed deprotection of the Boc-protected amine, thioester **2** to liberate AZD3409 **1** have been studied in a mixture of toluene and propan-2-ol. The reaction rate was found to exhibit a second-order dependence upon the HCl concentration. This behavior was found to have a degree of generality as the deprotection of a second Boc-protected amine, tosylate **3** to yield amine **4** using HCl, sulfuric acid, and methane sulfonic acid showed the same kinetic dependence. In contrast the deprotection of tosylate **3** with trifluoroacetic acid required a large excess of acid to obtain a reasonable rate of reaction and showed an inverse kinetic dependence upon the trifluoroacetate concentration. These observations are rationalized mechanistically in terms of a general acid-catalyzed separation of a reversibly formed ion–molecule pair arising from the fragmentation of the protonated *tert*-butyl carbamate.

Introduction

The *tert*-butoxycarbonyl (Boc) protecting group is widely used synthetically for the protection of amines and alcohols.¹ Two methods are commonly used to deprotect Boc-protected amines: either a large quantity of an acid such as trifluoroacetic acid or a relatively smaller quantity of a stronger acid such as hydrochloric acid.^{1,2}

AZD3409 **1**, isopropyl *N*-{5-({[(2*S*,4*S*)-4-(pyridine-3-ylcarbonyl)thiopyrrolidin-2-yl]methyl}amino)-2-[2-(4-fluorophenyl)ethyl]benzoyl}-*L*-methioninate, is a farnesyl transferase inhibitor undergoing investigation for the treatment of breast cancer and other tumors.³ The final stage in the synthetic sequence involves

the removal of a Boc protecting group from thioester **2**, isopropyl *N*-{5-({[(2*S*,4*S*)-1-(*tert*-butoxycarbonyl)-4-(pyridine-3-ylcarbonyl)thiopyrrolidin-2-yl]methyl}amino)-2-[2-(4-fluorophenyl)ethyl]benzoyl}-*L*-methioninate, with HCl (5 M) in propan-2-ol (IPA) (Scheme 1).⁴ During the development of this process the performance of the reaction was found to be extremely sensitive to the HCl usage. A kinetic investigation was undertaken to understand this sensitivity with a view to defining robust operating conditions. Additional studies of the deprotection of tosylate **3**, *tert*-butyl 4-[(4-methylbenzene)sulfonyloxymethyl]piperidine-1-carboxylate, to yield amine **4**, 4-[(4-methylbenzene)sulfonyloxymethyl]piperidine (Scheme 2), were undertaken to test the generality of the surprising findings of the initial investigation.

Results and Discussion

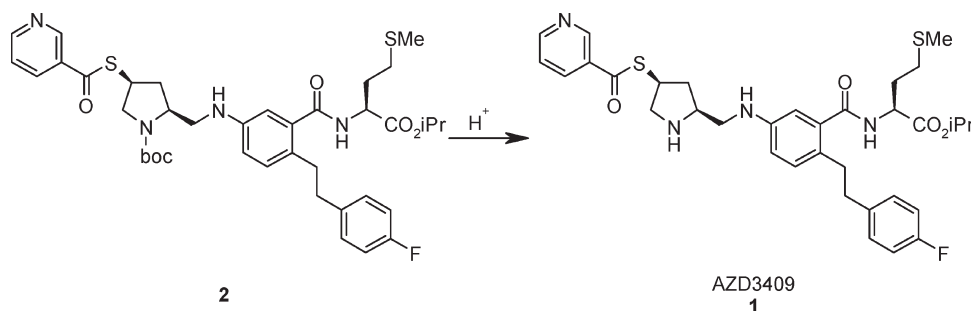
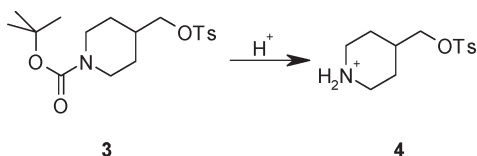
Kinetic Measurements. Reactions were profiled by HPLC at a range of temperatures and acid concentrations in toluene IPA (57% v/v). Raw HPLC peak area versus time data were normalized by using the toluene peak as an internal standard, corrected for any difference in response factor between

(1) (a) Carpino, L. A. *Acc. Chem. Res.* **1973**, *6*, 191–8. (b) Greene, T. W.; Wuts, P. G. M. *Protective Groups in Organic Synthesis*, 3rd ed.; Wiley: New York, 1999; p 518. (c) Kociński, P. *Protecting Groups*, 3rd ed.; Thieme: New York, 2004; p 461.

(2) (a) Mehta, A.; Jaohari, R.; Benson, T. J.; Douglas, K. T. *Tetrahedron Lett.* **1992**, *33*, 5441–5444. (b) Lin, L. S.; Lanza, T., Jr.; de Laszlo, S. E.; Truong, Q.; Kamenecka, T.; Hagmann, W. K. *Tetrahedron Lett.* **2000**, *41*, 7013–7016. (c) Gibson, F. S.; Bergmeier, S. C.; Rapoport, H. *J. Org. Chem.* **1994**, *59*, 3216–3218. (d) Strazzolini, P.; Melloni, T.; Giumanini, A. G. *Tetrahedron* **2001**, *57*, 9033–9043.

(3) (a) Stephens, T. C.; Wardleworth, M. J.; Matusiak, Z. S.; Ashton, S. E.; Hancox, U. J.; Bate, M.; Ferguson, R.; Boyle, T. *Proc. Am. Assoc. Cancer. Res.* **2003**, *44*, R4870. (b) Bell, I. M. *J. Med. Chem.* **2004**, *47*, 1869–1878.

(4) Abbas, S.; Ferris, L.; Norton, A. K.; Powell, L.; Robinson, G. E.; Siedlecki, P.; Southworth, R. J.; Stark, A.; Williams, E. G. *Org. Process Res. Dev.* **2008**, *12*, 202–212.

SCHEME 1. Deprotection of Thioester 2⁵SCHEME 2. Test Reaction System Used to Further Investigate the Removal of the *tert*-Butoxycarbonyl Protecting Group

the starting Boc-protected amine and the product and converted into concentration versus time data. Repetitive analyses of reaction samples that had been prepared for analysis demonstrated that the samples were stable for significantly longer times than were required to complete the analysis.

The work was carried out under a nitrogen atmosphere in a 100 mL jacketed reactor fitted with an overhead stirrer (Hastelloy pitched blade turbine), using an external circulating bath to maintain the reaction temperature. In a typical experiment tosylate **3** (3.70 g, 10.0 mmol) was suspended in toluene (12.89 g, 14.8 mL) and IPA (6.3 g, 8.0 mL) and the mixture was stirred until the tosylate dissolved. The solution was heated to 50 °C and a 5 M solution of HCl in IPA (3.0 mL, 15.0 mmol) was charged via a syringe. A 50 μ L sample was withdrawn, diluted into 1:1 acetonitrile:water (10 mL) and analyzed by HPLC. The experiment was maintained at 50 °C with periodic sampling for HPLC analysis. Typical concentration versus time profiles are shown in Figure 1.

Deprotection of Thioester 2. Deprotections of thioester **2** were studied with 3.2, 4, and 5 molar equiv of HCl in 57% v/v toluene IPA at 50 °C. Experiments were also undertaken at 30 °C with 5 and 6 molar equiv of HCl. The results are shown in Figures 1 and 2 and clearly show the conversion of thioester **2** to AZD3409 **1** without any evidence of a kinetically significant intermediate and that the reaction rate increases as the HCl concentration increases.

The widely accepted mechanism for the acid-catalyzed deprotection of a Boc-protected amine is a rapid pre-equilibrium protonation of the Boc group, followed by a rate-limiting fragmentation of the resultant protonated intermediate **5** (Scheme 3).⁶ In this mechanism it is assumed that the breakdown of the carbamic acid **6** initially produced by

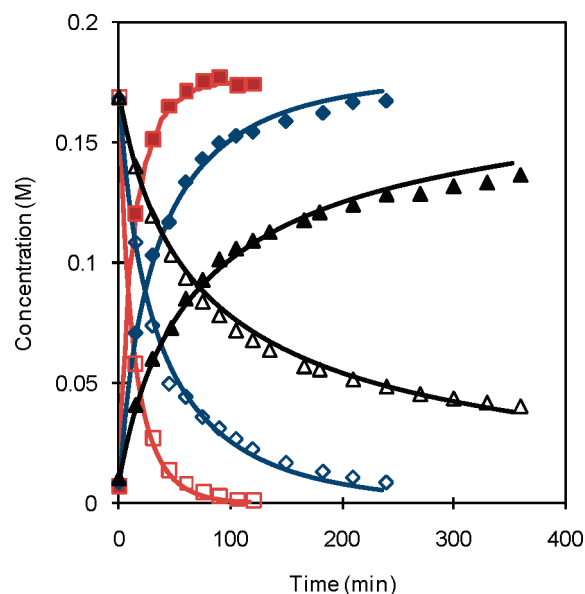


FIGURE 1. Influence of HCl usage on the deprotection of thioester **2** at 50 °C: 5 equiv of HCl thioester **2** (\square) and AZD3409 **1** (\blacksquare), 4 equiv of HCl **2** (\diamond) and **1** (\blacklozenge), and 3.2 equiv of HCl **2** (\triangle) and **1** (\blacktriangle).

the reaction is fast.⁷ For the reaction to be acid catalyzed the liberated *tert*-butyl cation must undergo further reaction to liberate a proton. In reality the deprotection reaction will consume an equivalent of acid through the protonation of the product amine. From this scheme it follows that the rate law for the deprotection reaction, assuming that little protonation of the Boc group occurs, is given by eqs 1 and 2.⁸

$$\frac{d[\text{P}]}{dt} = -\frac{d[\text{Boc}]}{dt} = -\frac{d[\text{H}^+]}{dt} = \frac{k_1[\text{Boc}]_T[\text{H}^+]}{(K_1 + [\text{H}^+])} \approx k_{\text{obs}}[\text{Boc}]_T[\text{H}^+] \quad (1)$$

$$k_{\text{obs}} = \frac{k_1}{K_1} \quad (2)$$

Simultaneous fitting of the experimental concentration versus time data to this rate law (eq 1) was undertaken using Micromath Scientist at each of the temperatures investigated.⁹ An initial [HCl] was calculated at each acid usage based on the

(5) The scheme depicts the isolated final product of the deprotection reaction. The actual product prior to the basic workup is expected to be the trication arising from the protonation of all of the basic sites (nitrogens) within the molecule.

(6) (a) Losse, G.; Zeilder, D.; Grieshaber, T. *Liebigs Ann. Chem.* **1968**, 715, 196–203. (b) Hudson, R. F.; Searle, R. J. G.; Mancuso, A. *Helv. Chim. Acta* **1967**, 50, 997–1002. (c) Lundt, B. F.; Johansen, N. L.; Vølund, A.; Markussen, J. *Int. J. Pept. Protein Res.* **1978**, 12, 258–268.

(7) Caplow, M. *J. Am. Chem. Soc.* **1968**, 90, 6795–6803.

(8) See the Supporting Information for the derivation of eq 1.

(9) Micromath Scientist, Version 2.0, from Micromath, St. Louis, Missouri. A sample model based on eq 1 for fitting three data sets simultaneously is given in the Supporting Information.

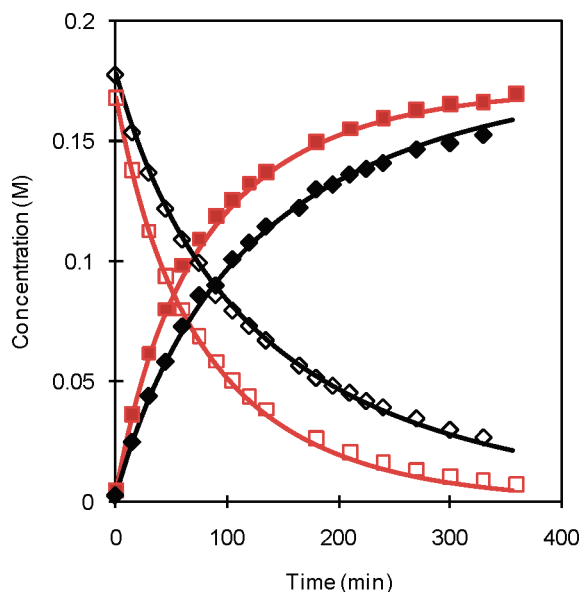
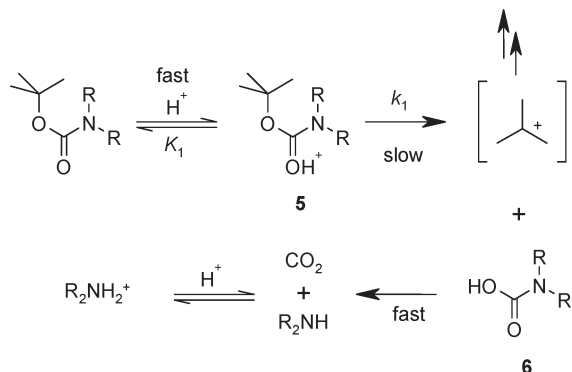
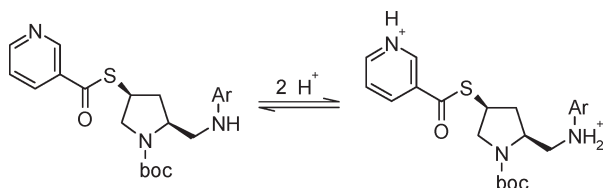


FIGURE 2. Influence of HCl usage on the deprotection of thioester **2** at 30 °C: 6 equiv of HCl thioester **2** (□) and AZD3409 **1** (■) and 5 equiv of HCl **2** (◇) and **1** (◆).

SCHEME 3. Expected Mechanism for the Acid-Catalyzed Deprotection of a Boc Protected Amine



SCHEME 4. Protonation of Thioester 2



assumption that 2 molar equiv of acid had been consumed in protonating the basic groups within thioester **2** (Scheme 4). The model also adjusted the [HCl] over the course of the reaction to allow for the protonation of the product amine. It was clear from the best-fit plots (for example, see Figure 3) that the experimental data were not described by the expected rate law.

Reanalysis of the kinetic profiles obtained at 50 °C gave the initial rate of reaction as a function of the initial free [HCl] and demonstrated that the initial rate of reaction did not show a first-order dependence upon the acid concentration (see the Supporting Information, Figure S1). The manner in which the

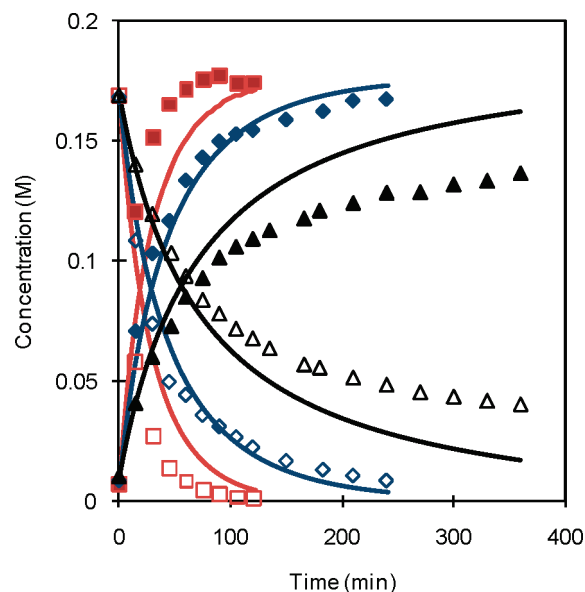


FIGURE 3. Best-fit plot for the acid-catalyzed deprotection of thioester **2** at 50 °C based on the expected mechanism: 5 equiv of HCl thioester **2** (□) and AZD3409 **1** (■), 4 equiv of HCl **2** (◇) and **1** (◆), and 3.2 equiv of HCl **2** (△) and **1** (▲).

plot deviated from linearity was suggestive of a higher order dependence. Consideration of the initial-rate data in terms of a second-order acid dependence (Figure 4) strongly suggested that the rate law for the deprotection reaction obeyed third-order kinetics, eq 3.

$$\frac{d[\text{P}]}{dt} = -\frac{d[\text{Boc}]}{dt} = -\frac{d[\text{HCl}]}{dt} = k_{\text{obs}}[\text{Boc}]_{\text{T}}[\text{HCl}]^2 \quad (3)$$

Fitting of the experimental data to this rate law was successful as shown by the best fit lines in Figures 1 and 2, giving rate constants of $5.7 \pm 0.4 \times 10^{-3}$ (50 °C) and $5.4 \pm 0.2 \times 10^{-4} \text{ M}^{-2} \text{ s}^{-1}$ (30 °C).

A brief investigation of the fate of the liberated *tert*-butyl cation was undertaken by GCMS. It was found that the main *tert*-butyl-derived product was the ether **7** derived from the trapping of the *tert*-butyl cation by solvent (IPA).¹⁰ Approximately 10% (based on GC area percent) of the *tert*-butyl group underwent trapping by chloride to generate *tert*-butyl chloride **8**, which is expected to slowly solvolyze under the reaction conditions.¹¹ Traces of isobutene **9**, arising from the elimination of a proton, were also seen (Scheme 5). No evidence was seen of the *tert*-butyl derivative of thioester **2** arising from the trapping of the *tert*-butyl cation by the product amine.

These results broadly support the hypothesis that the catalytic proton is regenerated by the onward reaction of the *tert*-butyl cation liberated during the deprotection. The formation of *tert*-butyl chloride represents a loss of acid term in the system, which will be most significant kinetically when close to stoichiometric acid is used for the deprotection. The inclusion of this pathway as an additional HCl loss term within the model used to fit the experimental data led to only a very slight improvement in the goodness of fit. The simple

(10) Dias, E. L.; Hettenbach, K. W.; am Ende, D. J. *Org. Process Res. Dev.* **2005**, *9*, 39–44.

(11) Grunwald, E.; Winstein, S. *J. Am. Chem. Soc.* **1948**, *70*, 846–54.

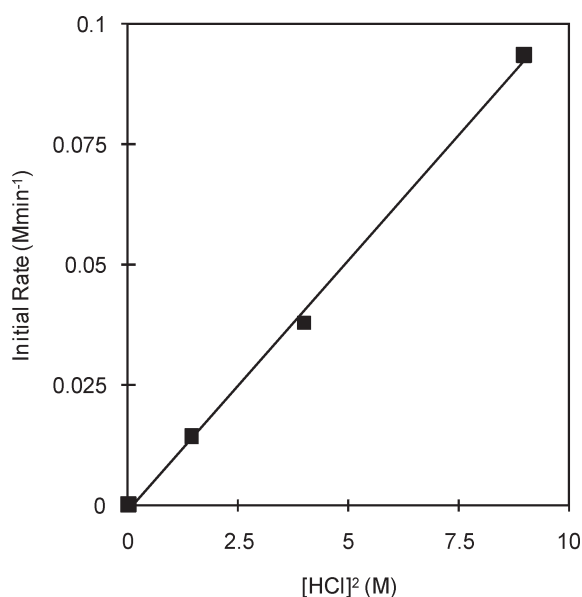
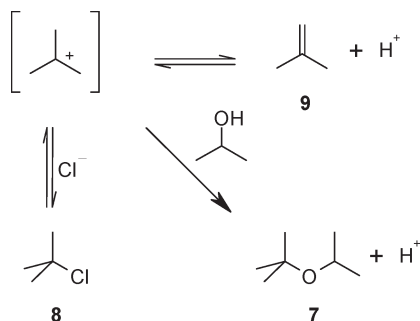


FIGURE 4. Dependence of the initial rates of thioester **2** deprotection upon the initial $[\text{HCl}]^2$ at 50 °C. The initial $[\text{HCl}]$ used allows for the HCl consumed by the protonation of the basic sites within **2**.

SCHEME 5. Fate of the *tert*-Butyl Group Liberated by the Deprotection of Thioester **2**



model, eq 3, was therefore used to generate the quoted rate constants.

The manufacturing process for AZD3409 **1** used a 0.2 molar equiv excess of HCl over the stoichiometric quantity required to protonate all the basic groups within AZD3409 **1**. A clear explanation for the extreme sensitivity of the process performance to the HCl charge used for the reaction was therefore provided by the observed second-order dependence in the deprotection kinetics of thioester **2** upon the $[\text{HCl}]$. Natural errors in charging reagents at scale could lead to a situation where the actual excess of HCl was lower than desired, leading to a very slow reaction that would take an unacceptably long time to meet the end of reaction criteria. Simulation of the process based on the observed rate law and experimental rate constants was undertaken to determine the size of the small increase in the HCl charge required to ensure robust process performance.

Deprotection of Tosylate **3.** The reactions of tosylate **3** were initially studied with the HCl in toluene IPA (57% v/v) system used for the deprotection of thioester **2**. Further studies were then undertaken with H_2SO_4 , methane sulfonic acid (MSA), trifluoroacetic acid (TFA), trichloroacetic acid, dichloroacetic acid, chloroacetic acid, and acetic acid as the

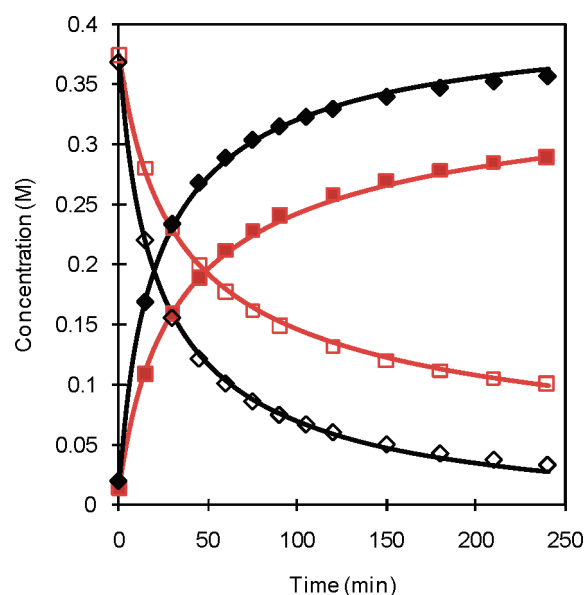


FIGURE 5. Best-fit plots for the deprotection of tosylate **3** with HCl at 50 °C: 1.5 equiv of tosylate **3** (\square) amine **4** (\blacksquare) and 1.1 equiv of **3** (\diamond) **4** (\blacklozenge).

TABLE 1. Temperature Dependence of the Third-Order Rate Constants for the Deprotection of Tosylate **3 with HCl in 57% v/v Toluene IPA**

$[\text{HCl}]$ (M)	temp (°C)	$10^4 k_{\text{obs}}$ ($\text{M}^{-2} \text{s}^{-1}$)
0.582	40	8.83 ± 0.02^a
0.427	50	
0.582	50	22.8 ± 0.2^b
0.582	60	75.0 ± 0.3

^aThe quoted errors are the 95% confidence limits of the best-fit rate constants arising from the fitting. ^bRate constant determined by simultaneously fitting the data from both of the experiments conducted at 50 °C.

catalyst. The deprotection with MSA was also studied in IPA with no toluene.

Initial experiments at 40, 50, and 60 °C with 1.5 molar equiv of HCl and 50 °C with 1.1 molar equiv of HCl gave clean reactions to liberate amine **4**. Fitting of the experimental concentration versus time data to a model based on eq 3 was successful (Figure 5)¹² to give the observed third-order rate constants listed in Table 1. This suggested that the unexpected second-order kinetic dependence upon the $[\text{HCl}]$ concentration observed in the deprotection of thioester **2** may be more general. The temperature dependence of the observed rate constants obeyed the Arrhenius equation (Figure 6) with an activation energy of $93 \pm 29 \text{ kJmol}^{-1}$ and a pre-exponential factor, A , of $2.5 \times 10^{12} \text{ M}^{-2} \text{ s}^{-1}$.

Deprotections with H_2SO_4 (1.8 molar equiv) and MSA (1.5 molar equiv) at 50 °C behaved similarly to the HCl-catalyzed reaction. Fitting of the experimental concentration versus time profiles for these deprotections to a model based on the experimentally determined rate law (eq 3, substituting the appropriate acid) was successful as shown in Figure 7. The best-fit rate constants are tabulated (Table 2) and compared to the rate constant for the HCl-mediated deprotection. Interestingly, the rate constants vary remarkably

(12) See Figure S2 in the Supporting Information for the best-fit plots at 40 and 60 °C.

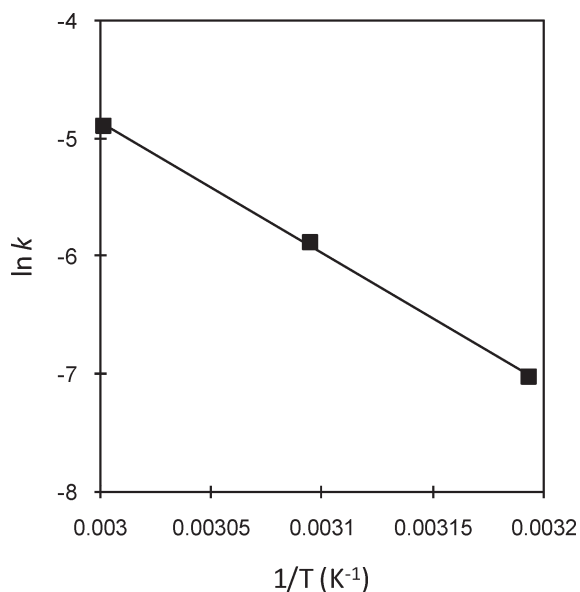


FIGURE 6. Arrhenius plot for the HCl-catalyzed deprotection of tosylate **3**: rate constant k in $\text{M}^{-2} \text{s}^{-1}$.

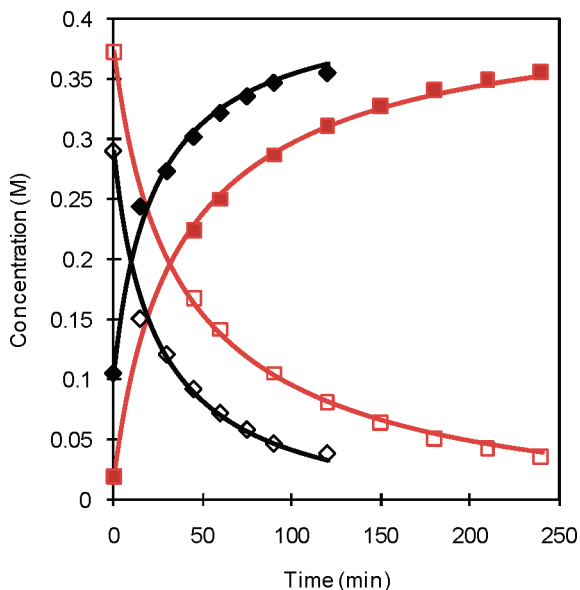


FIGURE 7. Best-fit plots for the deprotection of tosylate **3** with H_2SO_4 and MSA at 50°C : 1.8 equiv of H_2SO_4 , tosylate **3** (\square), and amine **4** (\blacksquare) and 1.5 equiv of MSA, **3** (\diamond) and **4** (\blacklozenge).

little as the acid is changed within this series. This relative insensitivity to the acid used makes the behavior observed with acids such as TFA all the more surprising (see below). In the case of MSA the rate constant for the deprotection reaction also appears to show little sensitivity upon changing the solvent from 57% v/v toluene IPA to IPA.¹³

The deprotection of tosylate **3** with 1.5 molar equiv of TFA was attempted at 50°C and abandoned after a week, as little reaction had occurred. This represents a dramatic change in rate relative to the MSA-catalyzed deprotection,

(13) See Figure S3 in the Supporting Information for a comparison of the best-fit plots for the MSA-mediated deprotection in IPA and 57% v/v toluene IPA.

TABLE 2. Third-Order Rate Constants for the Deprotection of Tosylate **3** with Different Acids in 57% v/v Toluene IPA at 50°C

acid	usage (molar equiv)	$10^3 k_{\text{obs}}$ ($\text{M}^{-2} \text{s}^{-1}$)
H_2SO_4	1.8	3.50 ± 0.02^a
HCl	1.1 and 1.5	2.83 ± 0.02
MSA	1.5	1.60 ± 0.03
MSA ^b	1.5	1.58 ± 0.10

^aThe quoted errors are the 95% confidence limits of the best-fit rate constants arising from the fitting. ^bRate constant for the deprotection of **3** in IPA.

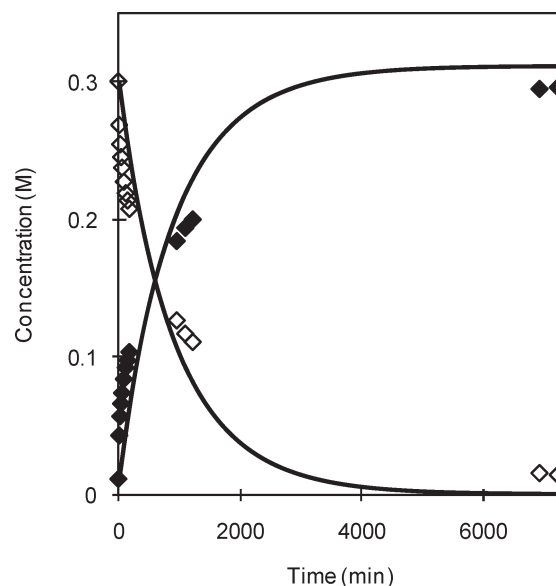
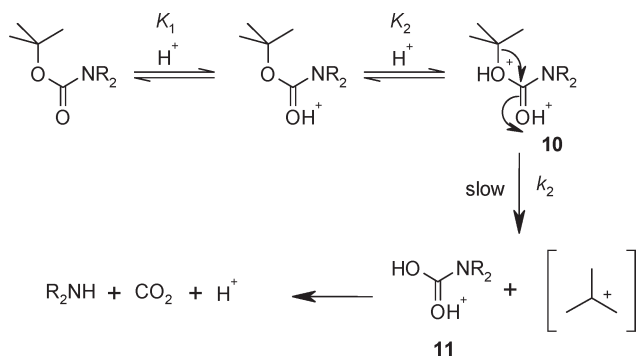
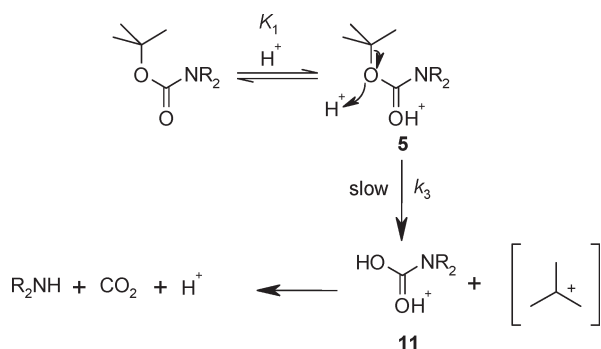


FIGURE 8. Best-fit plot for the deprotection of tosylate **3** with 10 molar equiv of TFA at 50°C : rate $\propto [\mathbf{3}][\text{TFA}]^2$, tosylate **3** (\diamond) and amine **4** (\blacklozenge).

which took 250 min to reach over 90% conversion. A slow observable reaction was obtained when 10 molar equiv of TFA was used, which took 5 days to give over 95% conversion at 50°C . The concentration versus time profile for this reaction does not fit to the same rate law (eq 3) as the deprotections of tosylate **3** catalyzed by H_2SO_4 , HCl, and MSA (see Figure 8) or to a rate law with a first-order acid dependence eq 1. Deprotections catalyzed by 10 molar equiv of trichloroacetic, dichloroacetic, chloroacetic, and acetic acid at 50°C were even slower with degradation of the tosylate **3** and amine **4** occurring on a similar time scale to the desired reaction.

Deprotection Mechanism. It is clear from the experimental data that the kinetic behavior of the deprotection reactions of thioester **2** and tosylate **3** catalyzed by H_2SO_4 , HCl, and MSA is not adequately described by the expected mechanism (Scheme 3), in which a pre-equilibrium protonation is followed by a rate-limiting fragmentation. Assuming that these acids are strong (fully dissociated), then the simplest explanation for the observed second order dependence of these deprotections upon the $[\text{HX}]$ ($\text{X}^- = \text{Cl}^-, \text{CH}_3\text{SO}_3^-, \text{HSO}_4^-$) is that a second proton is incorporated into the molecule before or during the rate-determining transition state. Two simple mechanisms can be written that include this second proton:

The first of these is an extension of the expected mechanism and involves the formation of a highly reactive diprotonated intermediate **10**, which then fragments to give a protonated carbamic acid **11** that loses CO_2 to give the

SCHEME 6. Mechanism for *N*-Boc Cleavage via a Diprotonated Intermediate**SCHEME 7. Mechanism for *N*-Boc Cleavage via a Bimolecular Acid-Catalyzed Fragmentation of a Protonated Intermediate**

protonated product amine (Scheme 6). Derivation of the rate law for a reaction according to this mechanism (treating the protonations as rapid pre-equilibria) gives eq 4, which may be simplified (eq 5) based on the assumption that very little of the diprotonated intermediate is formed (i.e., K_1K_2 is the dominant term in the denominator). This rate law has the same form as the experimentally observed rate law. However, experimental studies of alkyl carbamates in super acidic media at low temperatures have failed to find any evidence of diprotonated intermediates of the form of **10**,¹⁴ although protonated carbamic acids similar to **11** have been observed by NMR at low temperatures under strongly acidic conditions.¹⁵ It is therefore unlikely that this mechanism is operating under the significantly less acidic deprotection conditions.

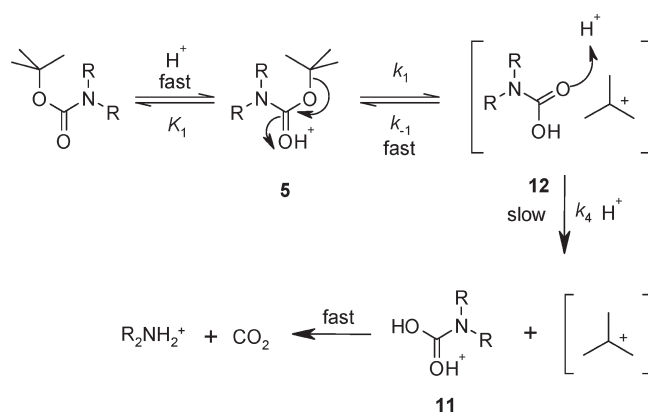
$$\frac{d[\text{P}]}{dt} = -\frac{d[\text{Boc}]}{dt} = -\frac{d[\text{H}^+]}{dt} = \frac{k_2[\text{Boc}]_T[\text{H}^+]^2}{(K_1K_2 + K_1[\text{H}^+] + [\text{H}^+]^2)} \quad (4)$$

$$\frac{d[\text{P}]}{dt} \approx \frac{k_2[\text{Boc}]_T[\text{H}^+]^2}{K_1K_2} \quad (5)$$

The second potential mechanism again builds on the expected mechanism and involves a bimolecular acid-catalyzed fragmentation of the protonated intermediate **5** to give the same protonated carbamic acid **11** as the first mechanism

(14) Olah, G. A.; Heiner, T.; Rasul, G.; Prakash, G. K. S. *J. Org. Chem.* **1998**, *63*, 7993–7998.

(15) Olah, G. A.; Calin, M. *J. Am. Chem. Soc.* **1968**, *90*, 401–404.

SCHEME 8. Mechanism for *N*-Boc cleavage via an Acid-Mediated Separation of an Ion–Molecule Pair

(Scheme 7). The rate law for this mechanism, eq 6, may be derived in an analogous manner to eq 4 and simplified to give a rate law, eq 7, with the same form as the experimentally observed rate law. While this mechanism avoids the generation of a relatively implausible intermediate, it does lead to the generation of two high-energy species in the rate-determining step, a protonated carbamic acid **11** and a *tert*-butyl cation, which make it less than satisfactory.

$$\frac{d[\text{P}]}{dt} = \frac{k_3[\text{Boc}]_T[\text{H}^+]^2}{(K_1 + [\text{H}^+])} \quad (6)$$

$$\frac{d[\text{P}]}{dt} \approx \frac{k_3[\text{Boc}]_T[\text{H}^+]^2}{K_1} \quad (7)$$

A third mechanistic possibility also exists,¹⁶ which is also a modification of the expected mechanism. In this proposal the protonated carbamate **5** undergoes a reversible fragmentation to give an ion–molecule pair **12** that rapidly recombines to regenerate the protonated carbamate **5**. The progress of the deprotection reaction is driven by a rate-limiting protonation of the carbamic acid within the ion–molecule pair, which drives the separation of the ion–molecule pair to give the protonated carbamic acid **11** and a *tert*-butyl cation. This is analogous to the behavior observed in the acid-catalyzed deprotection of trityl-protected amines.¹⁷ The rate law for this mechanism may be derived based on the assumption of a rapid pre-equilibrium protonation (eq 8). Simplification is possible if it is assumed that little of the protonated

(16) The authors would like to acknowledge the referees' helpful suggestions with respect to this mechanism.

(17) (a) Bleasdale, C.; Golding, B. T.; Lee, W. H.; Maskill, H.; Riseborough, J.; Smits, E. *J. Chem. Soc., Chem. Commun.* **1994**, 93–94. (b) Moisés, C. L.; Ibrahim, D.; Maskill, H. *J. Chem. Soc., Perkin Trans. 2* **2001**, 1748–1752.

(18) Clare, B. W.; Cook, D.; Ko, E. C. F.; Mac, Y. C.; Parker, A. J. *J. Am. Chem. Soc.* **1966**, *88*, 1911–1916.

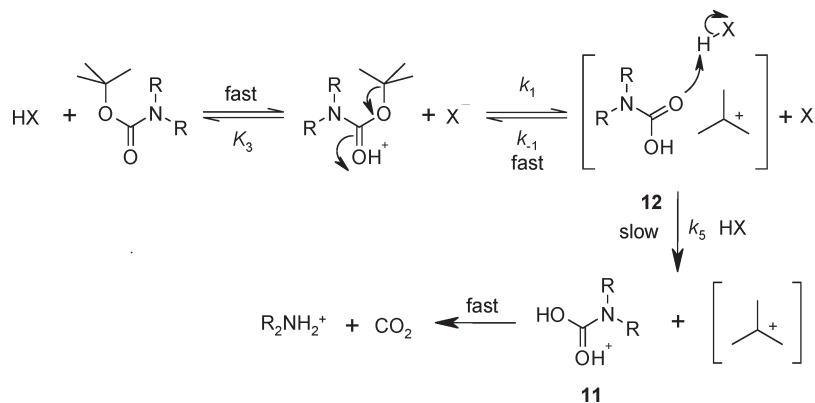
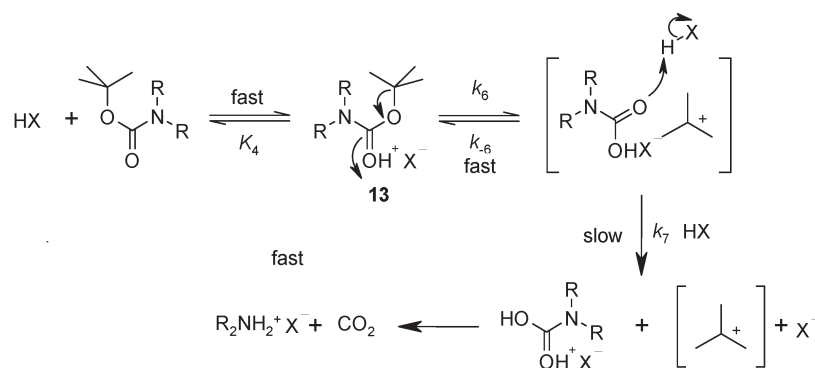
(19) Kolthoff, I. M.; Chantooni, M. K., Jr. *J. Phys. Chem.* **1979**, *83*, 468–474.

(20) Kanning, E. W.; Bobalek, E. G.; Byrne, J. B. *J. Am. Chem. Soc.* **1943**, *65*, 1111–1116.

(21) Perrin, D. D. *Ionisation Constants of Inorganic Acids and Bases in Aqueous Solution*, IUPAC Chemical Data Series No. 29, 2nd ed.; Pergamon: Oxford, UK, 1982.

(22) Serjeant, E. P.; Dempsey, B. *Ionisation Constants of Organic Acids in Aqueous Solution*, IUPAC Chemical Data Series No. 23, Pergamon: Oxford, UK, 1979.

(23) Chantooni, M. K., Jr.; Kolthoff, I. M. *Anal. Chem.* **1979**, *51*, 133–140.

SCHEME 9. Mechanism for *N*-Boc Cleavage via a General Acid-Catalyzed Separation of an Ion–Molecule PairSCHEME 10. Mechanism for *N*-Boc Cleavage via a General Acid-Catalyzed Separation of an Ion–Molecule Pair Resulting from the Fragmentation of an Intermediate Ion Pair

carbamate **5** is formed and that the collapse of the ion–molecule pair **12** back to the protonated carbamic acid is rapid compared to product formation. This gives rise to a rate law with the same form as the experimentally observed rate law (eq 9).

$$\frac{d[\text{P}]}{dt} = \frac{k_1 k_4 [\text{Boc}]_{\text{T}} [\text{H}^+]^2}{(k_{-1} + k_4 [\text{H}^+]) (K_1 + [\text{H}^+])} \quad (8)$$

$$\frac{d[\text{P}]}{dt} \approx \frac{k_1 k_4 [\text{Boc}]_{\text{T}} [\text{H}^+]^2}{k_{-1} K_1} \quad (9)$$

Differentiation between the three mechanisms discussed is not possible based on the available information, as all are described by the experimentally determined rate law. Additionally the mechanisms give rise to composite observed rate constants, which makes any mechanistic analysis based on activation parameters derived from the temperature dependence of the rate constants problematic. Of the three, the pathway containing an ion–molecule pair is the most appealing, as it does not require the formation of a species that has not been experimentally observed and has a reasonable precedent.¹⁷

The mechanism depicted in Scheme 8 and eq 8 predicts that the rate constant for all three acids should be equal, but, while similar, they show a trend to lower values as the strength of the acids decreases from H₂SO₄ to MSA. Furthermore, in the solvents used (IPA/toluene or IPA) the acids are expected to be relatively weak (i.e., not fully

TABLE 3. Comparison of Catalyst p*K*_a Values in Methanol, IPA, and Water

acid	p <i>K</i> _a MeOH	p <i>K</i> _a IPA	p <i>K</i> _a water
HCl	1.23 ^a	3.1 ^b	−6.3 ^a
H ₂ SO ₄	1.5 ^c		−3.6 ^d
MSA			−1.8 ^e
TFA			0.5 ^e
CCl ₃ CO ₂ H			0.5 ^e
CHCl ₂ CO ₂ H	6.4 ^a	7.8 ^f	1.29 ^a
CH ₂ ClCO ₂ H	7.7 ^a	9.2 ^f	2.86 ^a
CH ₃ CO ₂ H ^a	9.6 ^a	11.3 ^f	4.76 ^a

^aSee ref 18. ^bSee ref 19. ^cSee ref 20. ^dSee ref 21. ^eSee ref 22. ^fSee ref 23.

dissociated). Table 3 lists the acid strengths in methanol, IPA, and water of several of the catalytic acids used in this study. All become less acidic on transfer to methanol, and even more so in IPA. In particular, p*K*_a(HCl) = 3.1 in IPA, and hence in the concentrated solutions used for the kinetic studies, it will only be partially dissociated.

It is possible to write an analogous mechanism to that in Scheme 8 for catalysis by a weak acid (i.e., the acid is not fully dissociated), which makes the rate-limiting protonation to drive the separation of the ion–molecule pair a case of general acid catalysis, as shown in Scheme 9.

Such a mechanism leads to a rate law, eq 10, which may be simplified by assuming that only a small amount of the protonated intermediate is generated (i.e., $K_3[\text{X}^-] \gg [\text{HX}]$) and that the separation of the ion–molecule pair is slow relative to its collapse back to the protonated carbamate to give eq 11. This has an inverse dependence upon the

conjugate base of the catalytic acid, X^- , and is therefore not consistent with the rate law, eq 3, observed with HCl, H_2SO_4 , and MSA.

$$\frac{d[P]}{dt} = \frac{k_1 k_5 [\text{Boc}]_T [\text{HX}]^2}{(k_{-1} + k_5 [\text{HX}])(K_3 [X^-] + [\text{HX}])} \quad (10)$$

$$\frac{d[P]}{dt} \approx \frac{k_1 k_5 [\text{Boc}]_T [\text{HX}]^2}{k_{-1} K_3 [X^-]} \quad (11)$$

It is known, however, that ion-pair association constants for salts in IPA are very high (typically $> 10^3$).¹⁹ This suggests a modification to Scheme 9 in which the initial protonated intermediate exists as an ion-pair **13** rather than free ions, giving rise to Scheme 10. The rate law (eq 12) based on this scheme is in agreement with the observed rate law, eq 3. This mechanism is also consistent with the modest variation in observed rate constants for HCl, H_2SO_4 , and MSA. A high free concentration of the conjugate base of the catalytic acid does not build up as the reaction proceeds due to ion-pairing with the protonated amine produced by the deprotection reaction. In the case of thioester **2** the protonation of the basic sites within the molecule is also likely to lead to ion-pairing rather than free ions.

$$\frac{d[P]}{dt} \approx \frac{k_6 k_7 [\text{Boc}]_T [\text{HX}]^2}{k_{-6} K_4} \quad (12)$$

Finally, we consider the TFA-catalyzed deprotection of tosylate **3**. The reaction is extremely slow compared with the HCl-catalyzed reaction, for example, and even at 50 °C required a large excess (10 equiv) to achieve a reasonable conversion over 60 h. The high excess of TFA used in this experiment was such as to make it a significant part of the solvent system. Additionally it effectively meant that [TFAH] did not change during the reaction, meaning that it was not possible to distinguish effectively between rate laws with zero-, first-, and second-order dependencies upon [TFAH]. The analysis in Figure 8, however, shows that a simple rate law of the form of eq 3 was not able to provide an effective fit to the data, with the reaction becoming progressively slower than expected as it proceeded. A significantly better fit was achieved if an inverse dependence upon [TFA⁻] was included as in eq 11 (see Figure 9), with a composite second-order rate constant of $2.1 \pm 0.2 \times 10^{-7} \text{ M}^{-1} \text{ s}^{-1}$ at 50 °C. A rate law with a second-order dependence upon [TFAH] was used, as this had a degree of congruence with the behavior observed with the other acids and also gave a marginally better fit than rate laws with zero- or first-order dependencies upon [TFAH]. It is possible that the high [TFAH] was sufficient to provide stabilization to TFA⁻ through H-bonding (homohydrogen-bond formation), enabling TFA⁻ to exist as a “free” ion and hence adversely affect the pre-equilibrium protonation of tosylate **3** as the reaction proceeds.

Conclusions

This paper has demonstrated that removal of the Boc group routinely used for the protection of amines can exhibit a second-order kinetic dependence upon the concentration of the acid used to catalyze the reaction. The resultant third-order rate law has a degree of generality as it has proved applicable to two different substrates with three different acids. Naturally when

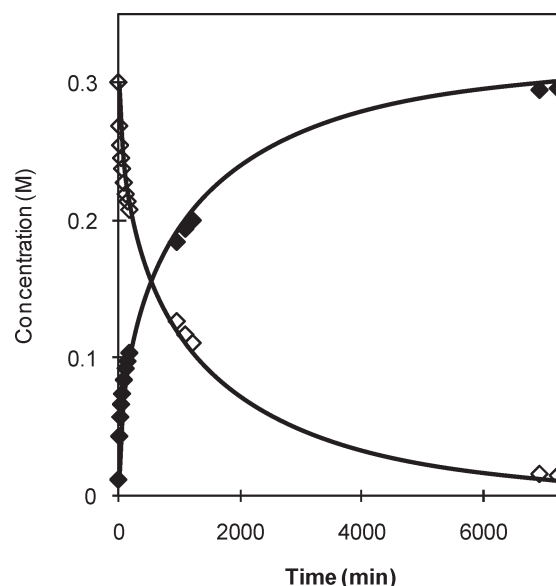


FIGURE 9. Best-fit plot for the TFA-catalyzed deprotection of tosylate **3** at 50 °C: rate $\propto [3][\text{TFAH}]^2/[\text{TFA}^-]$, tosylate **3** (\diamond) and amine **4** (\blacklozenge).

trying to develop efficient deprotection reactions this higher order kinetic dependence has significance, as it means the reaction tail will be extremely sensitive to the level of acid remaining toward the end of the reaction. Reaction rates among the stronger acids studied exhibit an order consistent with their expected order of acidities: $H_2SO_4 > HCl > MSA$. The differences are, however, only modest covering a range of a factor of 2. Weaker acids, such as TFA, and especially other, weaker carboxylic acids, require much larger concentrations and excesses in order to achieve practical reaction times. They appear to exhibit similar behavior, but it is modified by a reciprocal dependence upon the concentration of the conjugate base of the acid.

Mechanistically, a scheme consisting of a general acid-catalyzed separation of an ion–molecule pair arising from

TABLE 4. HPLC Method for Thioester **2** and AZD3409 **1**

column	Luna C-18		
	5 cm \times 2.0 mm, 2.0 μm		
temp	40 °C		
wavelength	265 nm		
flow	0.8 mL/min		
sample injection vol	3 μL		
run time	12 min		
post time	2 min		
Gradient			
time (min)	% water	% CH_3CN	1% trifluoroacetic acid soln
0	50	40	10
7	0	90	10
8	50	40	10
Sample Preparation: Take 50 μL of Reaction Mixture into a 10 mL Volumetric Flask, Dilute to Volume with 1:1 Aqueous Acetonitrile			
component		retention time (min)	
AZD3409 1		1.4	
toluene		1.7	
thioester 2		5.0	

TABLE 5. HPLC Method for Tosylate 3 and Amine 4

column	Zorbax SB C-18 5 cm × 2.0 mm, 1.8 μm
temp	40 °C
wavelength	256 nm
flow	1.5 mL/min
sample injection vol	3 μL
run time	8 min
post time	2 min

Gradient			
time (min)	% water	% CH ₃ CN	1% trifluoroacetic acid solution
0	85	5	10
0.2	85	5	10
5.2	0	90	10
6.4	0	90	10
6.5	85	5	10

Sample Preparation: Take 50 μL of Reaction Mixture into a 10 mL Volumetric Flask, Dilute to Volume with 1:1 Aqueous Acetonitrile

component	retention time (min)
amine 4	2.95
toluene	4.4
tosylate 3	5.1

the reversible fragmentation of the protonated Boc group is proposed to rationalize the observed kinetic behavior.

Experimental Section

Materials. Acetonitrile and propan-2-ol (IPA) used in the kinetic experiments were HPLC grade solvents, while the toluene was reagent grade. HCl in propan-2-ol was purchased as a 5.0 M solution from Acros and analyzed by titration prior to use. Acetic acid, chloroacetic acid, dichloroacetic acid, methane sulfonic acid, sulfuric acid, and trichloroacetic acid were of the highest commercial quality available and were used without further purification. HPLC grade trifluoroacetic acid was used for both the HPLC analysis and kinetic experiments.

Tosylate 3, *tert*-butyl 4-[(4-methylbenzene)sulfonyloxymethyl]-piperidine-1-carboxylate, was commercial material supplied by Isochem. Thioester 2, isopropyl *N*-{5-[[[(2*S*,4*S*)-1-(*tert*-butoxycarbonyl)-4-(pyridine-3-ylcarbonyl)thiopyrrolidin-2-yl]methyl]amino]-2-[2-(4-fluorophenyl)ethyl]benzoyl]-L-methioninate and AZD3409 1, isopropyl *N*-{5-[[[(2*S*,4*S*)-4-(pyridine-3-ylcarbonyl)thiopyrrolidin-2-yl]methyl]amino]-2-[2-(4-fluorophenyl)ethyl]benzoyl]-L-methioninate were prepared according to the previously described procedure.⁴ Its identity was confirmed by HPLC analysis (see Table 4) against an authentic sample.

Preparation of 4-Piperidylmethyl 4-Methylbenzenesulfonate (4) Methane Sulfonate Salt. A mixture of tosylate 3 (7.40 g, 1.0 molar equiv), toluene (48.1 mL), and propan-2-ol (3.7 mL) was stirred and heated to 50 °C under a nitrogen atmosphere to give a clear solution. Methane sulfonic acid (2.89 g, 1.5 molar equiv) was charged and the resultant two-phase system was maintained at 50 °C overnight. Reaction completion was confirmed by HPLC analysis (see Table 5). The reaction mass was cooled to 10 °C over 2 h and stirred at 10 °C for 2 h, after which the white crystalline solid was isolated by filtration under reduced pressure, washed with propan-2-ol (2 × 10 mL), and dried in vacuo at 40 °C. The unoptimized yield of amine 4 as its methane sulfonate salt was 3.2 g (43%): ¹H NMR (400 MHz, DMSO-*d*₆) δ (ppm) 1.31 (m, 2 H), 1.73 (d, *J* = 12.8 Hz, 2 H), 1.94 (m, 1 H), 2.35 (s, 3 H), 2.43 (s, 3 H), 2.84 (m, 2 H), 3.24 (d, *J* = 12.5 Hz, 2 H), 3.93 (d, *J* = 6.0 Hz, 2 H), 7.50 (d, *J* = 7.9 Hz, 2 H), 7.80 (d, *J* = 8.4 Hz, 2 H), 8.18 (br s, 1 H), 8.57 (br s, 1 H); ¹³C NMR (100.6 MHz, DMSO-*d*₆) δ (ppm) 21.1, 24.4, 32.6, 39.7, 42.5, 73.5, 127.6, 130.2, 132.2, 145.0; MS (ES) *m/z* (*M* + H⁺) 270.1166 vs 270.1158 calcd for C₁₃H₂₀NO₃S.

Acknowledgment. We thank Dr. G. E. Robinson, Dr. L. Ferris, Mrs. J. Cherryman, Dr. A. T. Bristow and Dr. I. C. Jones for discussions and for help with synthetic and analytical work.

Supporting Information Available: Derivation of eq 1, sample Micromath Scientist model file, plot of initial rate vs [HCl], for 2, best-fit plot for the deprotection of 3 at 40 and 60 °C, best-fit plot for the deprotection of 3 with MSA in IPA, and ¹H and ¹³C NMR spectra of compound 4. This material is available free of charge via the Internet at <http://pubs.acs.org>.